Capabilities of Result Visualization in LS-OPT® V4.1 - Demonstrated by Means of Industrial Problems

Katharina Witowski, Heiner Müllerschön
DYNAmore GmbH

Abstract

During the last decade the optimization software LS-OPT has been used for design optimization, for DOE-studies, for system identification and for stochastic investigations in many industrial projects. LS-OPT became over the years a highly sophisticated software tool with very effective and reliable optimization methodologies particular suitable for highly nonlinear problems.

This paper illustrates the capabilities of LS-OPT by means of several industrial applications. The focus is on the new post processing features of LS-OPT 4.1 such as visualizing results of multi-objective optimization, multiple load case optimization, sensitivity analysis and the visualization of curve data evaluated on the basis of meta-models. Of course, the objective and the setup of the optimization problems is discussed and demonstrated.

Keywords: LS-OPT, Optimization, Visualization, Pareto Optimal Solutions, Global Sensitivities

Introduction

This paper illustrates the capabilities of result visualization in LS-OPT 4.1 by means of industrial applications. The first example is a multi-objectives optimization with conflicting objectives considering two load cases. This results in a set of Pareto optimal solutions evaluated on the meta-model. The visualization capabilities for Pareto optimal solutions and curve data evaluated using meta-models are demonstrated.
The second example is a DOE study and focuses on the visualization of linear and non-linear sensitivities.

Optimization of a Crash Management System

Problem Description

This section describes the design of a bumper in a given constructed space. Two load cases are considered, the AZT crash repair test and the RCAR test, Figure 1. The objectives are to remove the impact energy by plastic deformation of the bumper and to reduce the mass of the bumper. The given constraints are a maximal force level of the barrier contact force for the AZT crash repair test and that the bumper has an extruded section. The ANSA Morphing Tool [2] is used as pre-processor in LS-OPT to modify the geometry from a starting design, and some sheet thicknesses are parameterized using LS-OPT. The crash simulations are performed using the LS-DYNA explicit FE-solver.

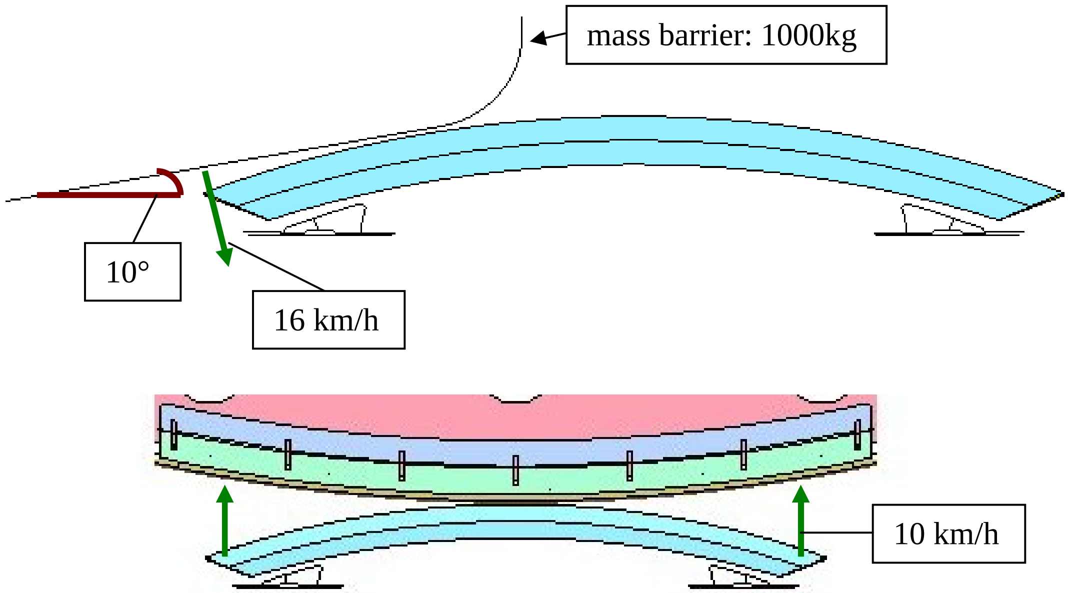

Figure 1: Load case AZT (top) and load case RCAR (bottom)

Optimization

Four morphing parameters are defined to modify the shape of the bumper, Figure 2. In addition, the sheet thicknesses of the five bumper parts are defined as design variables. Hence we get nine design variables in total.

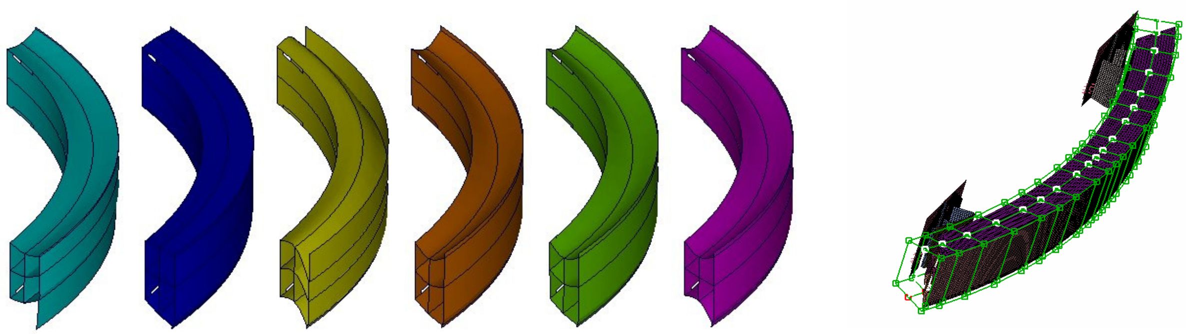

Figure 2: Shape variations realized with ANSA morphing tool

To optimize the energy absorption by plastic deformation of the bumper for the AZT crash repair test, the contact force between the barrier and the vehicle should be as close as possible to the maximal force level. Hence the sum of squares error between the calculated force curve and a target curve with a constant value, which is the given maximal force level, is considered.

For the load case RCAR, the maximal intrusion of the bumper is important. The intrusion is defined as the difference of the displacement of the center of mass of the vehicle and a node at the inner edge of the bumper.
The last objective considered is to minimize the total mass of the bumper.

A sequential meta-model based optimization is performed using LS-OPT. The genetic algorithm NSGA-II is used to find Pareto optimal solutions on the meta-model. Radial basis function networks are used to approximate the design space.

For details on the example, we refer to [4].

Visualization

This method results in a set of Pareto optimal solutions that the engineer has to investigate to select the solution that suits best to his application.

To determine conflicting objectives, the SOM (Self Organizing Map) plot is useful, see [3].
Component plots of the three objectives and the constraint are displayed in Figure 3. Cells with low values are colored in blue, cells with high values in red.

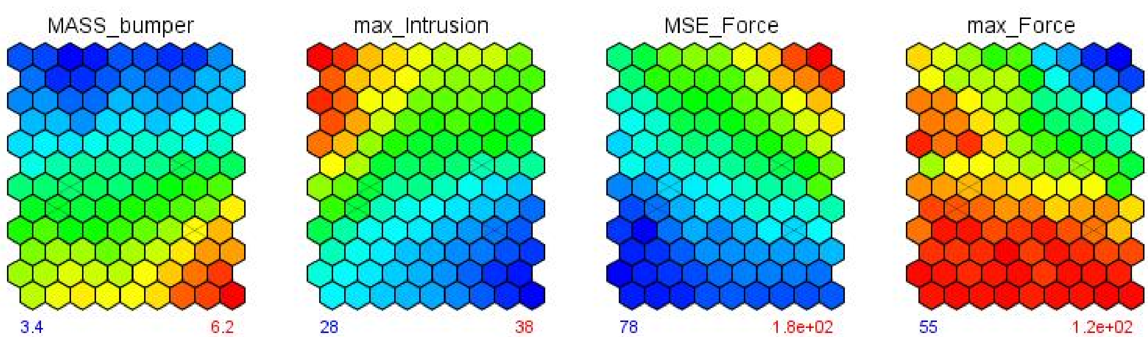

Figure 3: Self Organizing Map – component plot of objectives and constraint

The mass and the intrusion are conflicting, whereas the intrusion and MSE_Force are rather in agreement.

The Parallel Coordinate Plot helps to reduce the number of suitable solutions by restricting the ranges of objectives. Sliders can be moved up and down to limit the range of the objective values. In Figure 4, the upper bound for the mass is reduced. The blue bold lines are the remaining Pareto optimal solutions that are still within the defined target range for the mass.

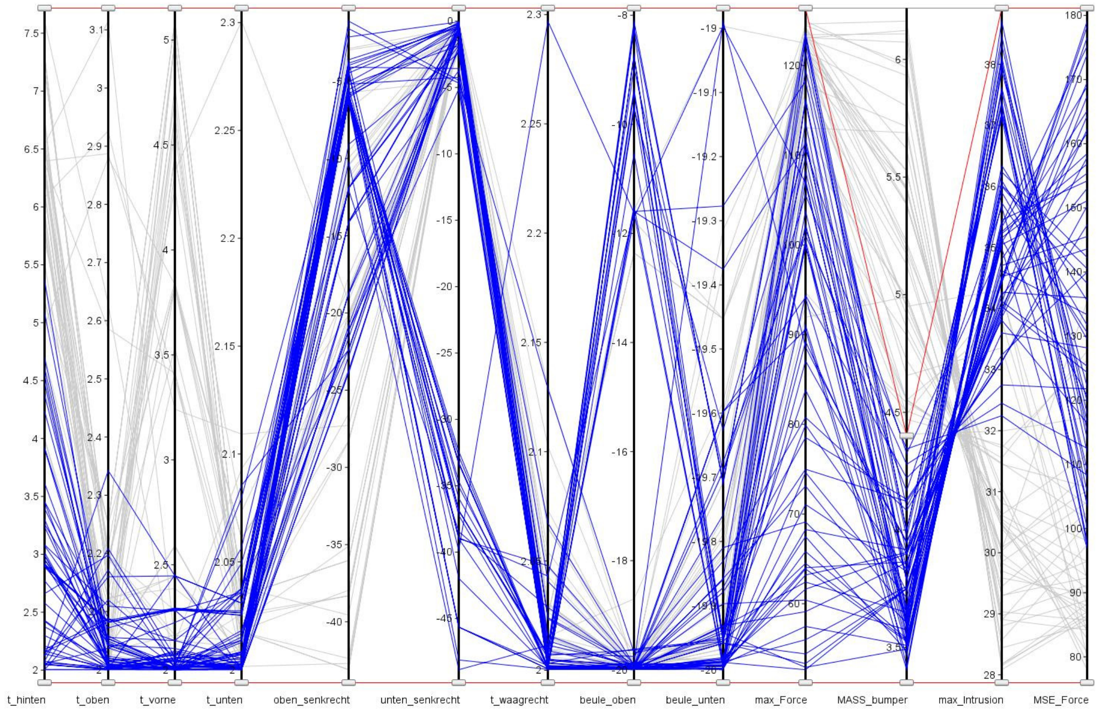

Figure 4: Parallel Coordinate Plot with constraint on the mass, the blue bold lines represent feasible points

In this example, one objective is to optimize the contact force curve. Figure 5 shows the computed force curves for all iterations with several coloring options. Since the Pareto optimal solutions are evaluated on the meta-model, there are no simulation runs available with the respective variable combinations.

LS-OPT 4.1 extends the idea of using meta-models to history curves, Figure 6 explains the approach. Hence a predicted history for any design point may be displayed. Figure 7 shows a Parallel coordinate plot with a selected Pareto optimal solution and the predicted history for the variable values of the selected point. That way the user gets an idea how the force curve for his selection looks like. All coloring options available for computed histories are also available for predicted histories. If predicted histories are colored by variable, curves for the whole range of the selected variable are displayed, Figure 8. This visualizes the effect of a single parameter on the curve.

After selecting some suitable points out of the set of Pareto optimal solutions, the design points may be stored in a .csv file that can be read as user-defined sampling in LS-OPT and hence verification runs for the predicted results can be performed.

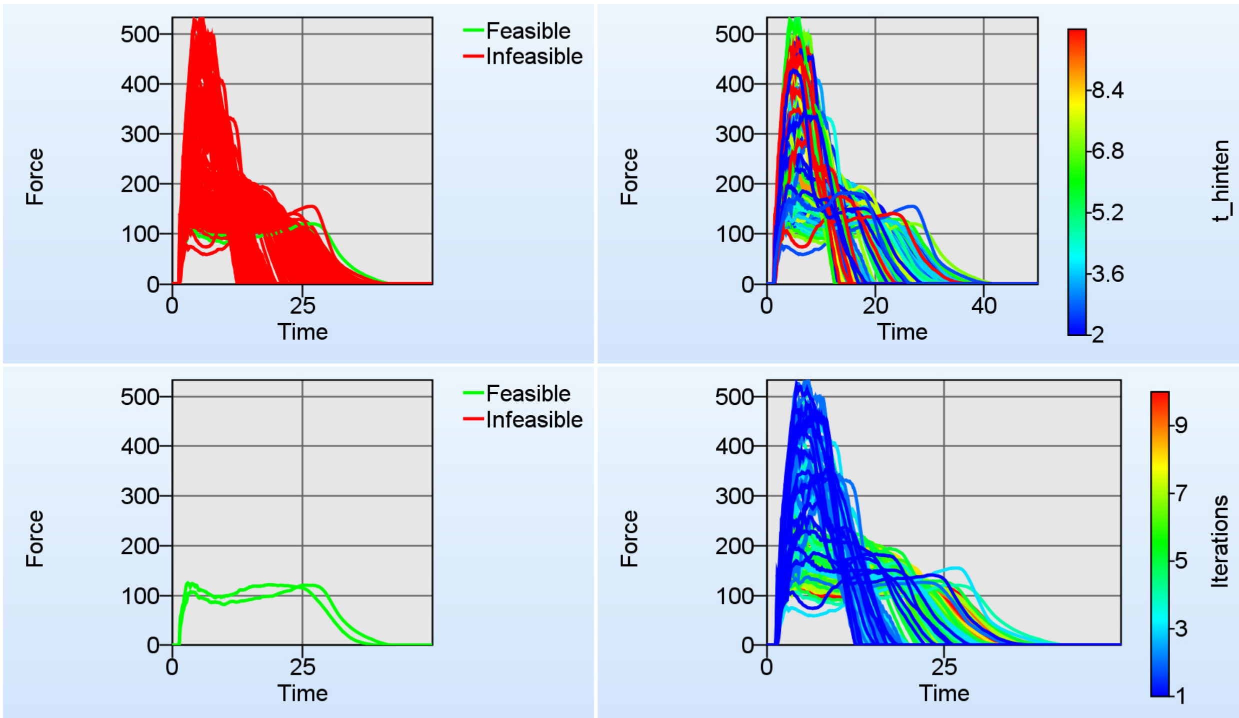

Figure 5: Computed history curves – all iterations – colored by feasibility (top left), colored by variable (top right), only feasible (bottom left), colored by iteration (bottom right)

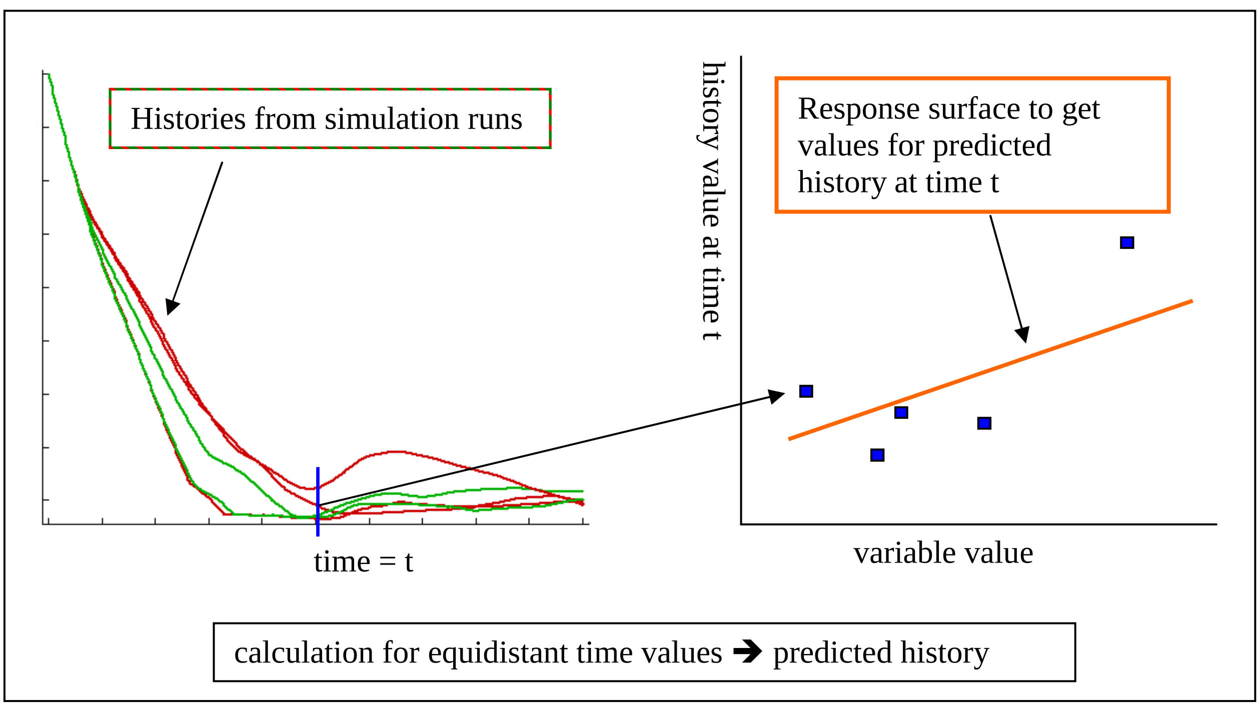

Figure 6: Predicted history curves – extension of meta-model approach on curve data. For each time value t a predicted history value for any specified variable combination can be calculated by using response surface approximations.

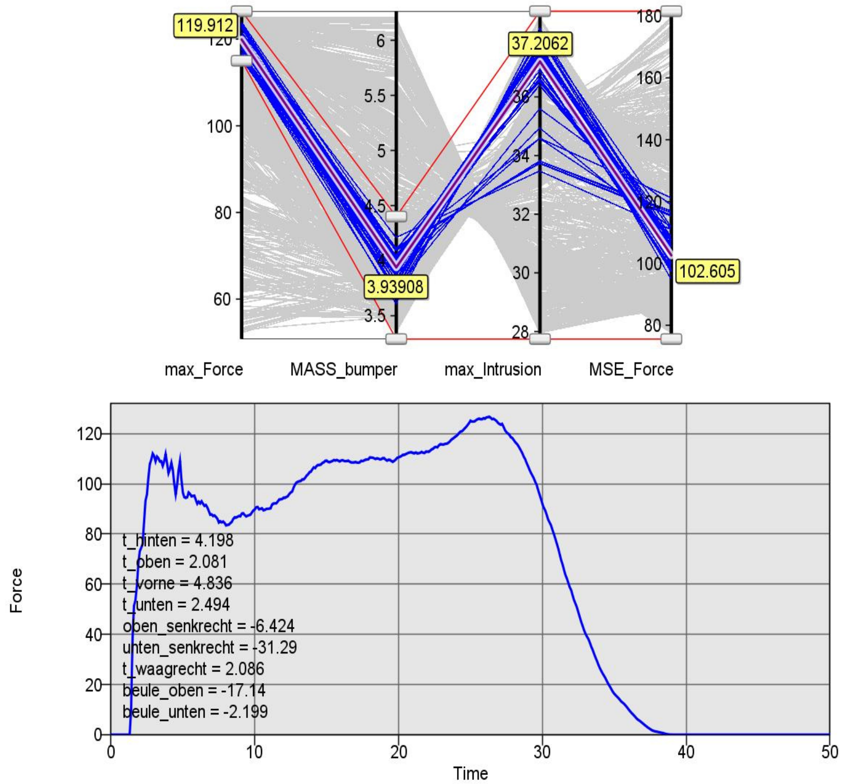

Figure 7: Parallel Coordinate Plot and Predicted History Plot with variable values evaluated from a selected Pareto optimal point in the upper PC-plot

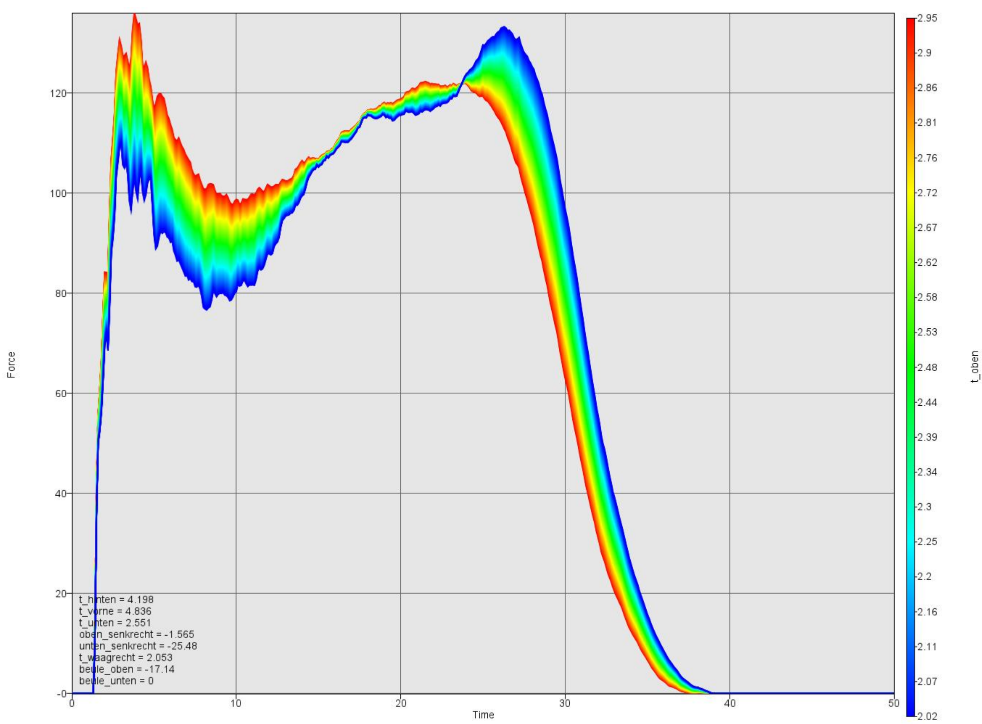

Figure 8: Predicted History curves colored by variable value

DOE Study of a Front Crash

Problem description

This section describes a DOE study of a frontal impact of a car on a rigid barrier, Figure 9. The finite element model is obtained from [6]. The design variables are the sheet thicknesses of the parts highlighted in Figure 10, the ranges of the variables are displayed in Table 1. The considered responses are the chest acceleration of the dummy, and forces evaluated at two cross sections, Figure 11. In addition, there is a constraint on the mass of the vehicle. 250 simulations are performed using the LS-DYNA explicit solver. The sensitivities are evaluated on RBF meta-models.

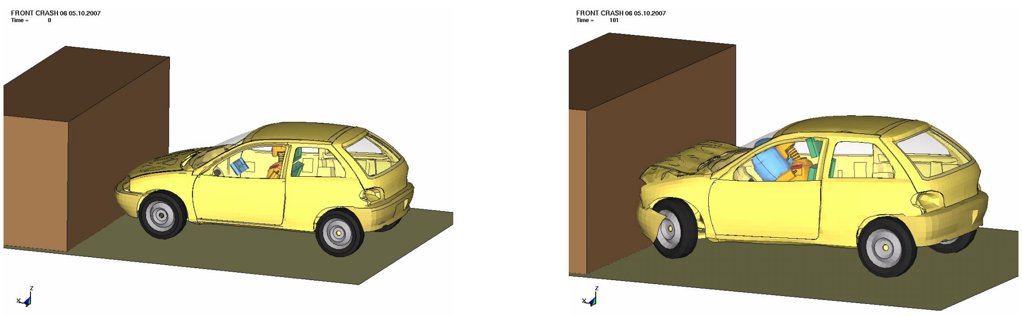

Figure 9: Frontal impact of a car on a rigid barrier, finite element crash model

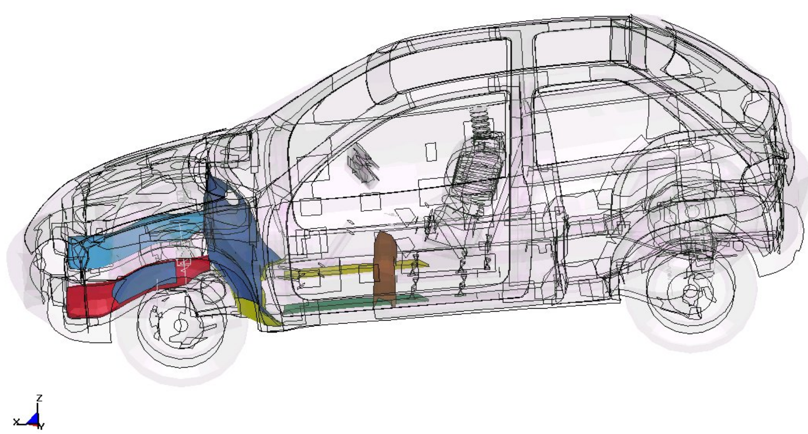

Figure 10: Design Variables – sheet thicknesses of highlighted rails

Variable	Lower bound	Upper bound
lb1	1.0	1.5
lb2	1.3	1.8
lb3	0.8	1.3
c1	0.8	1.3
c2	0.8	1.3
c3	1.0	1.5

Table 1: Design variable ranges

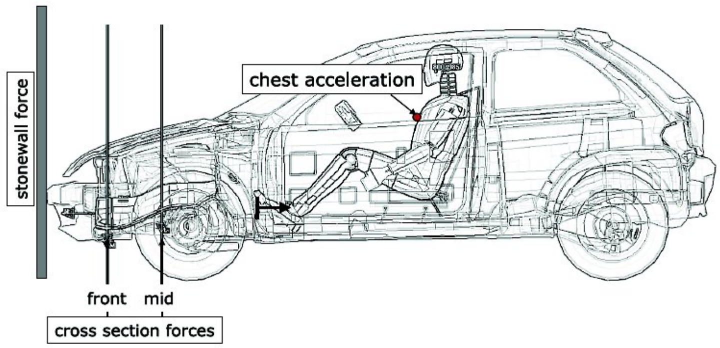

Figure 11: Evaluated responses – chest acceleration and cross section forces

Visualization

LS-OPT offers several visualization methods to determine the significance of design variables on responses. The approaches are explained in [5] and [7].

Figure 12 shows the correlation matrix with scatter plots, histograms and linear correlation coefficients. The correlation coefficients are determined using the values from the simulations. The correlation coefficients indicate that variable *lb1* has a strong effect onto the section forces, whereas all variables are insignificant on the chest acceleration. The linear effect of *lb1* on the section forces is also visible in the scatter plots.

Figure 13 displays linear ANOVA results calculated on the meta-model. For the chest acceleration, the ANOVA results are not meaningful because of the large red error bars. For the cross section forces, the ANOVA results are in agreement with the results obtained from the correlation matrix.

These two approaches only consider linear correlations. If there is e.g. a quadratic correlation of a variable and a response, this could cause misleading results if only linear correlation is considered, hence LS-OPT 4.1 calculates also non-linear sensitivities. It is recommended to look at both approaches and compare the results.

Figure 14 displays global sensitivities according to Sobol. Each bar represents the contribution of a particular variable to the variance of the respective response. *lb1* has the strongest effect on the whole problem, and again on the section forces, but here, *lb1* also has a strong effect on the chest acceleration. Table 2 compares the total variances of the responses. The variance of the chest acceleration is quite small. This explains that linear ANOVA and the correlation matrix show small sensitivities here.

For both linear and non-linear sensitivities, *lb1* is the most sensitive variable on *SECFORC_front_resp*, but the percentage in comparison to the other variables is higher for the non-linear correlation. This can be explained by the quadratic correlation displayed in Figure 15, which is not detected completely by the linear correlation.

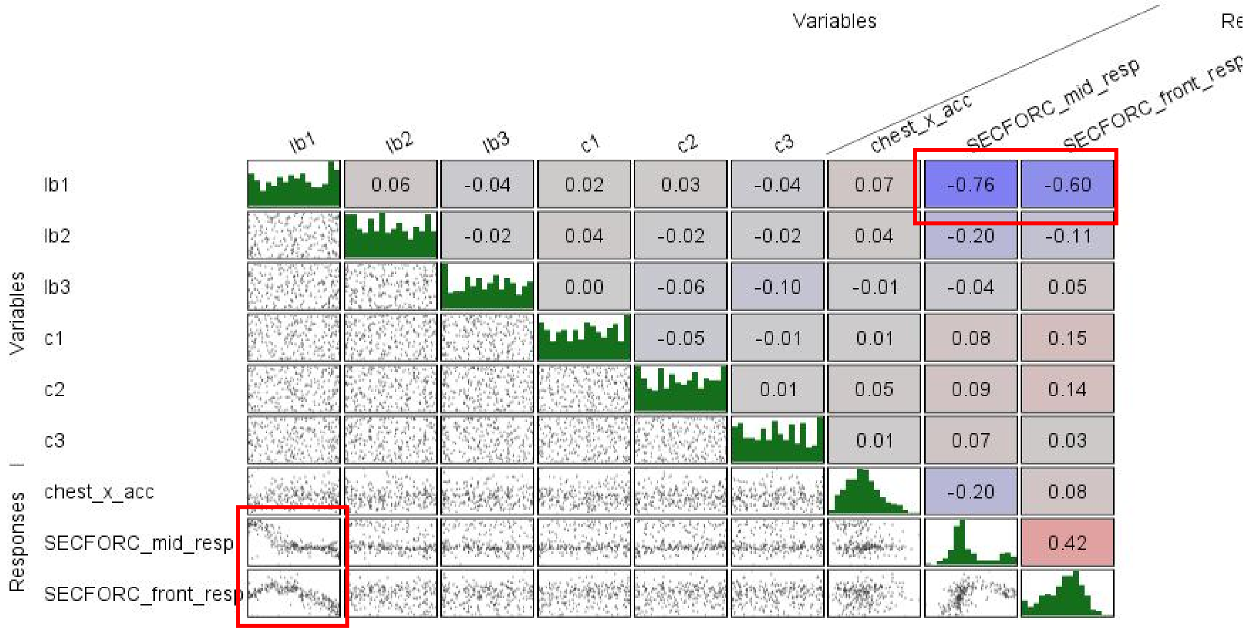

Figure 12: Correlation Matrix – Scatter plots, histograms and linear correlation coefficients

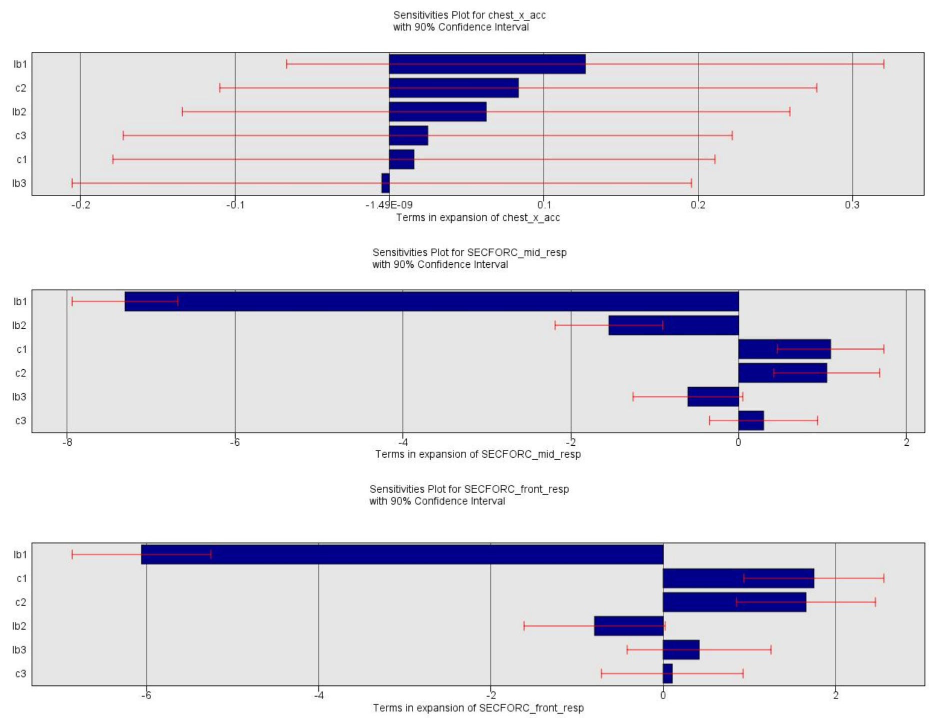

Figure 13: Linear ANOVA of chest acceleration and cross section forces sorted by significance; length of bars indicate sensitivity of variable with respect to responses, red error bars mark scatter in the data.

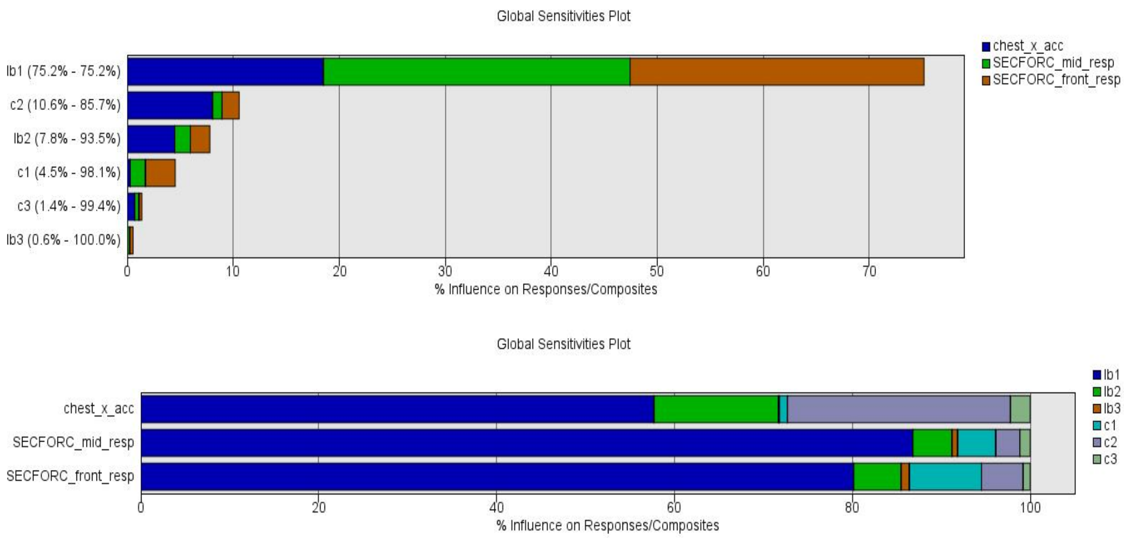

Figure 14: Global (non-linear) Sensitivities – Sobol indices; upper plot: percentaged contribution of variables to variance of responses indicates significance of variables on selected responses, variables sorted by significance, lower plot: alternative depiction for significance of variables on respective response

	Total variance
chest_x_accel	0.0013
SECFORC_mid_resp	5.16
SECFORC_front_resp	4.73

Table 2: Total variances of objectives

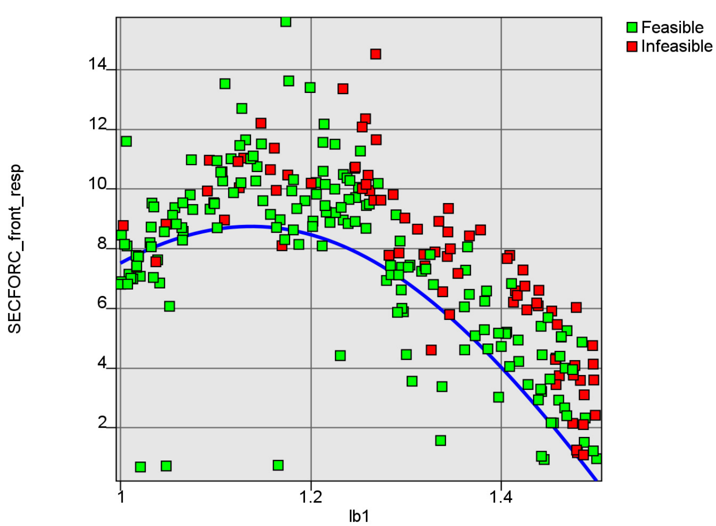

Figure 15: Surface Plot – response SECFORC_front_resp vs. variable lb1

Figure 16 displays the Interpolator Plot for all variables against the objectives and the constraint. It visualizes 2D sections of the response surfaces in a matrix. Constraints and the predicted value for the selected design point may be displayed. This is suitable for comparing the influence of variables on several responses, or to find feasible regions in the design space.

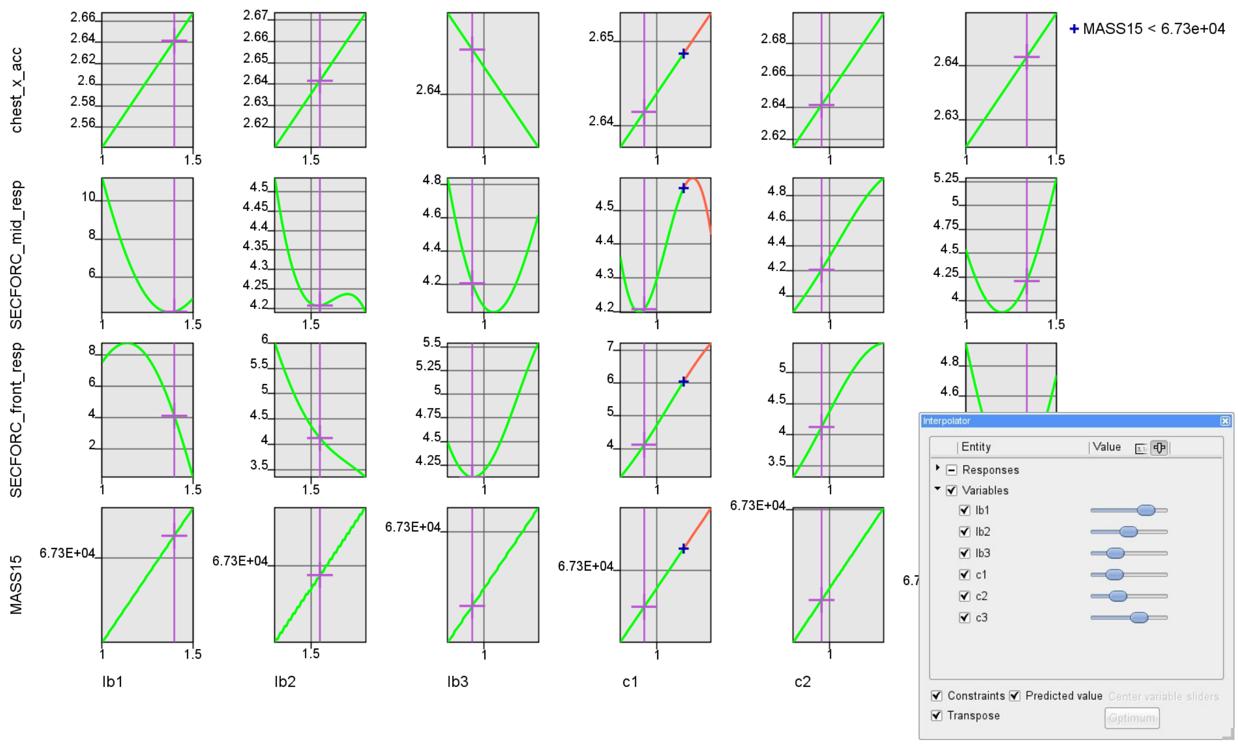

Figure 16: Interpolator Plot with constraint visualization and predicted value for design point selected using variable sliders

Summary

The post-processing features of LS-OPT 4.1 have improvement in visualizing results of multi-objective optimization, the visualization of curve data and the visualization of sensitivities.

The SOM plot completes the visualization of high dimensional data together with the Tradeoff Plot, the Parallel Coordinate Plot and the HRV Plot that are already available in LS-OPT 4.0.

Another new approach is the extension of the meta-models on curve data, this offers the possibility to visualize predicted histories. Improvements are also made in the visualization of sensitivities and features to visualize non-linear sensitivities were added.

References

[1] Stander, N., Roux, W., Goel, T., Eggleston, T., Craig, K., LS-OPT® User's Manual, Version 4.0, Livermore Software Technology Corporation, Livermore, 2009
[2] ANSA version 12.1.3 User's Guide, BETA CAE Systems S.A., 2007
[3] Witowski, K., Liebscher, M., Goel, T., Desicion Making in Multi-Objective Optimization for Industrial Applications – Data Mining and Visualization of Pareto Data, 2009
[4] Feuerstein, M., Witowski, K., Muellerschoen, H., Optimization of a Crash Management System considering Multiple Load Cases using ANSA and LS-OPT, 2008
[5] Reuter, U., Liebscher, M., Global sensitivity analysis in view of nonlinear structural behaviour, 2008
[6] National Crash Analysis Center, George Washington University, http://www.ncac.gwu.edu
[7] Saltelli A. et al., Global Sensitivity Analysis – The Primer, John Wiley & Sons Inc., 2008